INVESTIGATION AND TAGUCHI OPTIMIZATION OF FIRE RESISTANCE IN ULTRA-HIGH PERFORMANCE CONCRETE (UHPC) PRODUCED USING MINERAL ADDITIVES

SELÇUK MEMİŞ[1*] , **ALİ ALSHAAB RAMROOM** [2]
[1] *Kastamonu University, Department of Civil Engineering, 37100, Kastamonu, Turkey*
[2] *Department of Materials Science and Engineering, Institute of Science, Kastamonu University, 37100, Kastamonu, Turkey*

In this study, the effects of silica fume (SF), fly ash (FA) and granulated blast furnace slag (GBFS) on the design and fire resistance properties of ultra-high performance concrete (UHPC) were analyzed using the Taguchi L16 method. Samples were exposed to temperatures of 300 °C, 450 °C and 600 °C. The composition of the UHPC was: sand/binder ratio = 1, water/binder ratio = 0.19, Polycarboxylate superplasticizer (PCE) /binder ratio = 3.5%, pozzolanic (SF, FA and GBFS)/binder ratio = (0, 10, 15, 20)% and steel fibers = 1% by volume, and a Taguchi L16 program was prepared that consisted of 240 samples (40x40x160mm). The high-temperature properties of the UHPC samples were evaluated. Because several mixtures could withstand a temperature of 450 °C, it was determined that the losses were more effective when the highest temperature reached was greater than or equal to 600 °C, and the twelve mixtures are damaged by breaking them up. When the actual values obtained in the verification test were examined, it was determined that the results were sufficient for the compressive and flexural strength and physical properties of the concrete under various heating conditions and the Taguchi optimization was successfully implemented.

Keywords: *Ultra-high performance concrete (UHPC); Cement; Steel fibers; Polycarboxylate ether-based superplasticizers (PCEs); Compressive strength; Taguchi Method; Fire resistance*

1. Introduction

Concrete is a construction material that plays a basic and important in our modern world [1]. Moreover, concrete is a material that has advantages such as durability properties and a low cost to create the desired shape and size. [2–11] However, concrete also has durability issues such as corrosion of the reinforcements, alkali-silica reaction, sulfate attack and the freeze-thaw effect, which is associated with cracks caused by mechanical, thermal and chemical stress of structures. This not only accelerates the deterioration of concrete structures and shortens their service life, but also increases the life-cycle cost as careful monitoring and periodic maintenance and rehabilitation are required. Conventional concrete is not suitable for harsh environmental applications [12]. Since the 1980s, significant research and development efforts to improve the mechanical and durability properties of concrete have led to the evolution of ultra-high performance concrete (UHPC), with applications in the construction of buildings that require higher strength concrete with higher corrosion resistance [13–16]. The initial aim of the UHPC production process was to develop a single material that has minimal disadvantages compared to conventional concrete and has many properties including pore voids, micro cracks and superior load-bearing capacity [17].

UHPCs were first introduced in France in the 1990s and are a relatively new class of advanced cementitious composite materials that exhibit much higher mechanical and durability properties than conventional concrete [12]. UHPC is an advanced cementitious material typically created with a low water/binder (w/b) ratio and high fineness additives without any coarse aggregates [13–15]. UHPC typically consists of a combination of Portland cement (PC), fine aggregate, SF, a high proportion of high-range water reducers (HRWR) for high viscosity (self-leveling) and micro steel fibers [12,18,19]. While ACI-239 defines manufactured UHPC as a high compressive strength concrete material with a strength of 150 MPa and greater [20], ASTM C1856 defines it as a cementitious mixture with specified strength, ductility and toughness requirements and specific compressive strength of at least 120 MPa [21]. UHPC, which has higher strength than conventional and high strength concretes, is a material that exhibits performance superior [22]. It has mechanical and durability properties such as compressive strength of at least 120 MPa, a tensile strength of 5–15 MPa and flexural strength of 30–40 MPa [14,23]. These improved mechanical and durability properties have led to the development of smaller structural components/elements as well as the improved durability of structures [24]. The construction of smaller elements is associated with a reduction in shipping, mold, labor and maintenance costs. The high strength of UHPC guarantees sustainability through the construction of slim and durable designs. The high durability of UHPC results mainly maintenance costs [25,26]. Briefly, UHPC can be from its resistance to all types of corrosion, which extends the design life of a project and reduces characterized by its machinability, high strength and

* Autor corespondent/*Corresponding author*,
E-mail: smemis@kastamonu.edu.tr

toughness, low porosity and superior durability [24].

Due to the low w/b ratio (0.15–0.25) that reduces the capillary pores in its production and disconnects them, UHPC cannot move in the structure of gas and liquids. Additionally, it is a stronger and more homogeneous material as the diameter of the aggregates decreases. The steel additive used in UHPC prevents the occurrence of micro and macro cracks and increases the shear stress, flexural strength and ductility [20]. Similar to other types of concrete, the mechanical performance of UHPC changes when exposed to fire. Because the density of UHPC is extremely high, it can cause high water pressure when exposed to fire. Additionally, this situation causes deterioration and destruction of the concrete structure. However, this issue can be overcome if polypropylene fibers are used when the burning or melting process occurs since these fibers form capillary pores. To achieve this, a connection between the transition zones around the fibers and between the matrix and aggregates in the transition zones (which reduces the vapor pressure), is required. The use of polypropylene fibers can limit the explosive tendency of the UHPC and reduce the depth of propagation [27–31]. However, its pore structure is vulnerable to explosive spread in case of fire exposure [24].

Since the generation of UHPC, extensive focus has been placed on its fresh and rheological properties [19,32–36], mixture designs [16,18,37–39], fiber–matrix bond properties [40,41], mechanical properties [42–45], dimensional stability [46–53], hydration and microstructure [51,54–57] and its structural design and applications [58–61], as well as microstructure characterization [11,62,63]. Additionally, investigations on the durability of UHPC (including chloride ion permeability, carbonation, steel fiber corrosion and fire resistance) have been conducted [64–66].

To reduce the cement content without significantly compromising the mechanical strength, high-volume substitutes for cement can be created using materials such as fly ash (FA), ground granulated blast furnace slag (GGBS) and silica fume (SF). It is stated that this substitution ratio is 20–35% (by volume%) of GGBS, 10–30% of FA and 15–30% of SF in UHPC mixtures [18,38,39]. However, most UHPCs contain SF and silica dust. SF is a reactive powder with pozzolanic properties. Silica powder is an inert powder that is mainly used to increase the density of the cementitious matrix. The effects of SF on the hydration and microstructure of UHPCs are due to the fact that SF dominates the hydration process at lower w/b ratios [37]. Previous studies have shown that the typical SF content used in the UHPC mix is approximately 20%–30% by mass of cement-based materials.

Because of widespread terrorism, which has increased in recent decades, governments and researchers have been focusing on explosion and fire protective structures. UHPC is regarded as a desirable material for such structures. Portland cement has been recently been investigated as a new additive in several nanomaterials in the production of UHPC. It is a high strength, ductile material that is formulated by combining SF, quartz flour, fine silica sand, HRWR, water and steel or organic fibers. However, fire or high temperatures remain a major threat to all types of concrete, including UHPCs [11]. Although concrete is an excellent fire-resistant building material, if the free moisture content is below 3% to 4%, an explosive spill will not occur due to its low thermal conductivity and high thermal capacity. However, with low amounts of free water, the virtual absence of capillary pores may result in the concrete becoming more prone to explosive spill due to increased vapor pressure and a non-uniform thermal gradient during heating [12]. The aim of this study was to investigate the strength and mass-loss rates of UHPC produced using the L16 matrix with SF, FA and GBFS additives from industrial wastes at a low w/b ratio (0.19). Moreover, the effectiveness of the Taguchi method in UHPCs exposed to high temperatures was also investigated.

2. The Taguchi Method

The Taguchi method is a statistical technique developed by Genichi Taguchi during the 1950s as an optimization process procedure [67]. Taguchi's approach to parameter design provides the design engineer with a systematic and efficient method for determining near optimum design parameters for performance and cost. The initial concept of Taguchi that must be discussed is the "noise factors". Noise factors are viewed as the cause of variability in performance, including why products fail. The signal-to-noise ratio (S/N) is used to evaluate the quality of the product [68].

The S/N measures the level of performance and the effect of noise factors on performance and provides an evaluation of the stability of the performance of an output characteristic. Target values may be:

Smaller is better, this is chosen when the goal is to minimize the response. The S/N can be calculated as given in Equation (1) for the smaller the better.

$$\frac{S}{N} = -10 * \log_{10}\left(\frac{1}{n}\sum_{i=1}^{n} Y_i^2\right) \quad \text{.....(1)}$$

Larger is better, this is chosen when the goal is to maximize the response. The S/N is calculated as given in Equation (2) for the larger the better.

$$\frac{S}{N} = -10 * \log_{10}\left(\frac{1}{n}\sum_{i=1}^{n} \frac{1}{Y_i^2}\right) \quad \text{.....(2)}$$

Nominal is better, this is chosen when the goal is to target the response and it is required to base the S/N on standard deviations only. The S/N is calculated as given in Equation (3) for the nominal the better.

$$\frac{S}{N} = -10 * \log_{10}\left(\frac{1}{n}\sum_{i=1}^{n} (Y_i - Y_0)^2\right) \quad \text{.....(3)}$$

In Eqs. (1)–(3), Y shows the measured value of each response. When variability occurs, it is because of the physics that are active in the design and the environment that promotes the change. Noise factors can be classified into three groups [69]:

- External noise factors: sources of variability that originate from outside the product.
- Unit-to-unit noise: since no two manufactured components or products are exactly alike.
- Internal noise: due to deterioration, aging and wear incurred during storage and use.

The objective is to select the most suitable combination of control parameters so that the product or process is most robust with respect to the noise factors. The Taguchi method utilizes orthogonal arrays from the design of experiments theory to study a large number of variables using a small number of experiments. An orthogonal array significantly reduces the number of experimental configurations to be studied. Furthermore, the conclusions drawn from small-scale experiments are valid over the entire experimental region spanned by the control factors and their settings.

There are ten steps in a systematic approach to the use of Taguchi's parameter design methodology. These steps are [70]:

- Problem recognition and formulation.
- Select the quality characteristic.
- Select the design or process parameters.
- Classify the design parameters.
- Determine the levels.
- Identify the interactions.
- Choose the appropriate orthogonal array.
- Conduct the experiments.
- Perform the statistical analysis.
- Perform a confirmatory experiment and implement the results.

3. Materials and Methods

3.1. Materials:

During the UHPC production process, washed silica sand (Fig.1) at 0–2 mm sieve size obtained from the city of Kastamonu was used. The particle size distribution of the sand used in the study, which had a fineness module of 2.14 according to ASTM C 136 [71], is shown in Fig. 2. Additionally, PC in the form of type 1 (CEM II/A-M (P-L) 42.5R) (OPC) according to TS EN 197-1 standard [72] and with a cement specific weight of 2.94 gr.cm-³ and Blaine surface area of 4191 cm².gr-1 was used. The SF used in the concrete production was obtained from the Antalya Eti-Mine Electro-Ferrochrome Plant and was used according to ASTM C 1240 standard [73]. The SF specific weight used was 0.55–0.65 gr.cm-³ and the Blaine surface area was 23.36 m².gr-1. The other pozzolanic materials used were FA and GBFS. The FA was used as a mineral admixture which was classified as

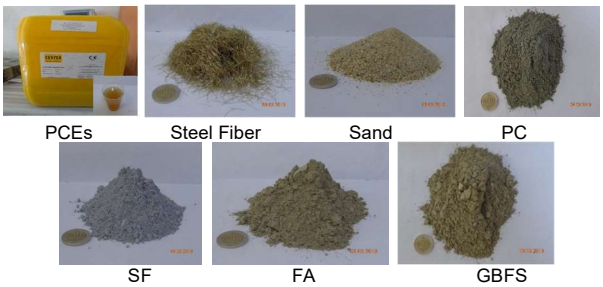

Fig. 1 - The materials used in the production UHPC

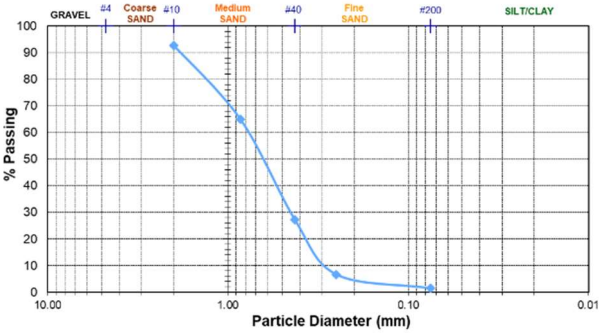

Fig. 2 - The Sieve analysis of sand used

a V-type according to TS EN 197-1 [72], and it was also classified as F-type according to ASTM C 618 [74]. The GBFS was provided by the Ereğli Iron & Steel Works Company in Kdz. Ereğli, Turkey. The chemical compositions of GBFS and FA are shown in Table 2. For this research, PC conforming to the TS EN 197-1 [72] standard requirements was obtained from the Bolu Cement Industry Inc., Turkey. The detailed physical and chemical properties of the cement used in this experiment are shown in Table 1.

Table 1
The chemical composition, physical and mechanical properties of the using materials

Chemical composition (%)	**PC**	***FA***	***SF***	***GBFS***
CaO	63.59	1.77	0.44	.37.79
SiO_2	20.90	61.81	80.9	35.09
Al_2O_3	5,.53	9.54	0.34	17.54
Fe_2O_3	3.70	7.01	0.55	
MgO	1.76	2.56	5.23	5.75
Na_2O	0.18	2.43	0.35	0.74
K_2O	0.41	0.99	4.5	0.28
SO_3	0.73	0.31	-	0.19
Cl	0.0027	-	0.13	
Free CaO	2.56	-	2.70	
Physical and mechanical properties				
Comp. str. 2 days (MPa)	17.9			
Comp. str. 7 days (MPa)	31.7			
Comp. str. 28 days (MPa)	45.9			
Specific gravity	2.94	2.76	0.55-0.75	2.95
Initial setting time (min.)	177			
Final setting time (min.)	233			
Volume stability (mm)	1			
Blaine value ($cm^2.gr^{-1}$)	4191			
90 µm passing (%)	98.8			
32 µm passing (%)	88.5			

Steel fibers with a diameter of 0.15 mm, length of 13 mm, specific gravity of 7.8, a tensile strength of 3000 MPa and modulus of elasticity of 200 GPa were used. Polycarboxylate ether-based superplasticizers (PCEs) (Chryso® Lab Bet 8109) were adsorbed electrostatically to the cement surface with negatively charged carboxylic acids on the polymer surface. Due to this absorption, polyethylene glycol side chains [75] were used as superplasticizers in this study because they were stretched towards the water phase to provide an effective cement dispersing effect

3.2. Mix Design and Specimens Preparation

In this study, the design of the mixture was determined using the Taguchi L16 matrix. Each mixture was assigned a code (Table 2) with a specified letter identifier. A total of 16 groups of mixtures were prepared using the Taguchi method (Table 3), which included an orthogonal array L16 (4^3) that showed all factors and levels.

Table 2
The considered levels for each parameter in Taguchi design of experiment

Parametres	Code	Level			
		1	2	3	4
SF	S	0%	10%	15%	20%
FA	F	0%	10%	15%	20%
GBFS	G	0%	10%	15%	20%

Table 3
L16 array has been suggested by Taguchi method for 3 parameters at 4 levels

	Mixture	Parameters			
		Cement (%)	SF (%)	FA (%)	GBFS (%)
1	Reference	100	0	0	0
2	S0F10G10	80	0	10	10
3	S0F15G15	70	0	15	15
4	S0F20G20	60	0	20	20
5	S10F0G10	80	10	0	10
6	S10F10G0	80	10	10	0
7	S10F15G20	55	10	15	20
8	S10F20G15	55	10	20	15
9	S15F0G15	70	15	0	15
10	S15F10G20	50	15	10	20
11	S15F15G0	70	15	15	0
12	S15F20G10	55	15	20	10
13	S20F0G20	60	20	0	20
14	S20F10G15	55	20	10	15
15	S20F15G10	55	20	15	10
16	S20F20G0	60	20	20	0

In all the UHPCs produced in this study, the pretesting mixtures and cement dosage determined by the literature were kept constant at 1000 kg.m^{-3} [38,45,76–80]. Additionally, the w/b ratio was applied as 0.19 [29,35,45,80,81] and the PE/binder ratio was 3.5% [39,45,77]. While the blends had a sand/binder ratio of 1/1 (by weight), the number of steel fibers were kept constant at 1% by volume [32,34,80,82] in the same volume. The w/b ratio was adjusted to 0.2 for the control mixture only [29,45,76,83]. The effect of the sand and reinforcing fibers on the properties of the mixtures were examined in the context of choosing the best ratio used in the study. The mixes prepared in the concrete mixer were moved sideways with the bucket to align the fibers as much as possible and were filled into prismatic molds of 4x4x16 cm in size (Fig. 3). Additionally, within the scope of this study, the path followed at the laboratory stage was as follows:

- Preparation of the materials: Dry sand, FA and GBFS were kept at 105°C for 24 hours, thus, the materials were kept dry by removing moisture (Fig. 1).
- Mixing of the materials: The materials were mixed in a 10-liter bowl of an ÖZAK planetary mixer (LTC 320 model, 1100W) (Table 4) and were set aside after the mixing process.
- Mixing process: This type of mixing is generally performed specifically for the UHPC used in this study. The mixtures were prepared by following the mixing process (Table 4) specified by Torregrosa (2013) [77] for UHPC production.

Table 4
Mixing process of the study

Min	Process	Aspect	
0-1	Sand and binder mixing	Dry	
1-3	Adding water and 50% PCE	Dry - Plastic	
3-4	Stop the mixer	Plastic	
4-6	Mixing after adding the left over PCE	Plastic - Fluid	
6-7	High speed mixing	Fluid	
7-10	Mixing after adding steel fiber	Fluid	

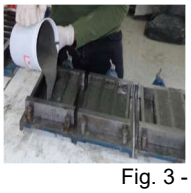

Fig. 3 - UHPC casting and test process

Temperature and humidity are important factors for improving the mechanical properties of UHPC, and these properties can be further improved through the use of heat curing regimes that accelerate the early strength of the concrete [1,84]. UHPC samples were removed from the molds 24 hours after the casting process was completed, and they were maintained until the day of the experiment by applying standard water curing (23.0 + 2.0°C) as specified by ASTM C192 [85].

3.3. Test Procedures

Compressive strength and flexural strength tests, which are among the hardened state

properties, were conducted on samples that underwent 28 days of curing. The tests were conducted using an experimental process according to the BS EN 196-1 [86] standard. Samples of 40x40x160 mm were placed horizontally on two supports that were spaced 100 mm apart. To assess the flexural strength, a vertical load application was initiated using a loading cylinder on the upper surface of the prism and was loaded at a rate of 50 ± 10 $N.s^{-1}$ until breakage occurred. To determine the compressive strength of the UHPC samples, the tests were performed on two parts obtained from the flexural strength test. For this purpose, a maximum capacity of 250K brand UTEST LC815 brand cement tester (Fig. 1) was used. According to the obtained force (Fr), the flexural strength was calculated using the equation $Rf = (1.5\ Fr\ L).b^{-3}$. Conversely, the compressive strength test was applied at a loading speed of up to 2400 ± 200 $N.s^{-1}$ to each one of the pieces that were broken during the flexural strength test and the compressive strength value was calculated with the help of the sample breaking load. Additionally, the density and void ratios were determined according to the ASTM C642 [87] standard. This was also useful for developing the conversion data for the mass and volume of the concrete, which aided in determining the concrete specifications and revealing variations in different locations.

The fire resistance test was conducted after 28 days. Before heating, a drying treatment is generally required to control explosive spalling [28]. A mechanically ventilated oven was used to dry the paste and mortar specimens at 105°C for 24 hours (Fig. 1). The samples were subjected to an elevated temperature in an electric furnace (Fig. 3). The samples were heated at a rate of 5°C/min until the following temperatures were reached: 300°C, 450°C and 600°C [88]. Once the test temperatures were reached, the samples were maintained at these temperatures for one hour to ensure the homogeneity of the thermal field in the sample [89]. At the end of each interval, the power was shut off and the oven was returned to room temperature. The mechanical tests were performed in a non-heated environment.

4. Results and Discussion

4.1. Compressive and Flexural Strengths

The compressive strength and flexural test results were determined at 28th days at standard water curing (SC) [86] as shown in Fig. 4, Fig. 5 and in Fig. 6.

FA and GBFS were used as mineral additives in the UHPC mixtures (Fig. 6). It was determined that the compressive strength caused a decrease with the increase of its content and in the use of SF. It is known that the use of FA decreases the strength of concrete at an early age and increases the strength

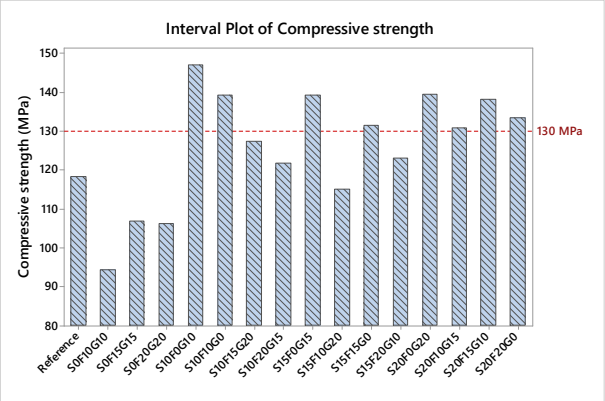

Fig. 4. Compressive strength range

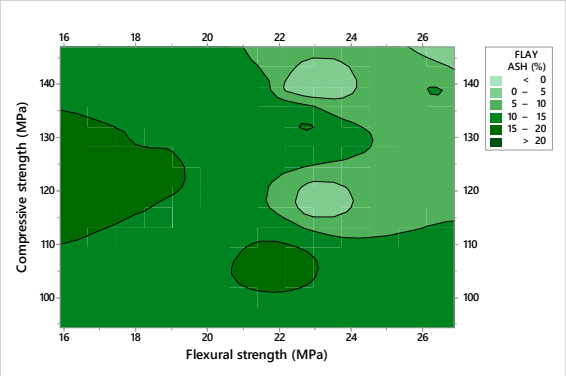

(a) FA

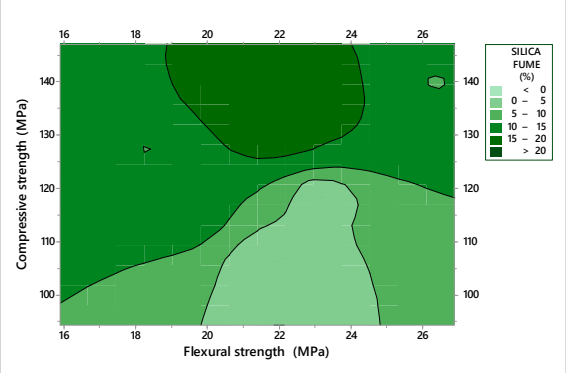

(b) SF

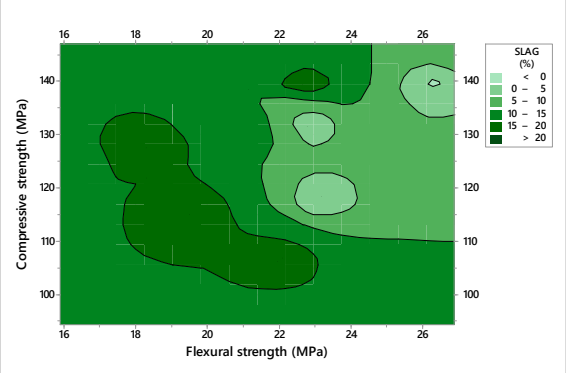

(c) GBFS

Fig. 5 - Contour plot of mineral admixtures impact on compressive strength results

in later stages of concrete maturation [52]. Maltais and Marchand (1997) reported that at a curing temperature of 20°C, depending on the cement replacement level and FA type, the compressive strength of an FA mortar mixture takes 25–50 days to reach the reference value [54]. This indicates that pozzolanic reactions of FA become dominant after 28 days of use in cement replacement under standard water curing conditions [55]. Increasing the FA addition to the UHPC resulted in a decrease in the total hydration of the system [56] and the FA activity was maintained at a lower level compared to the cement activity, resulting in a decrease in the strength at the 28th day curing values.

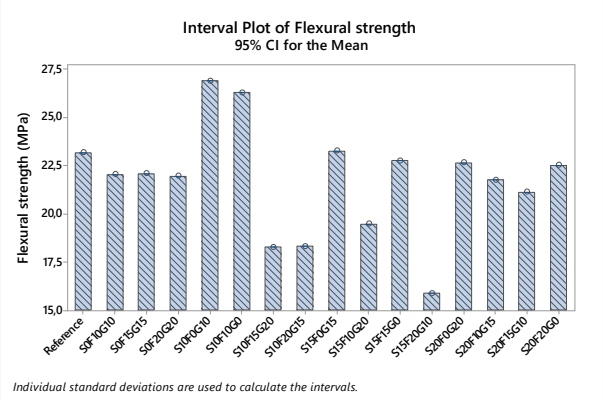

Fig. 6 -The flexural strength range

A similar decrease in strength was observed in the GBFS addition, and the results revealed that the FA and GBFS mineral additives caused a loss of strength after a certain rate in the UHPCs. However, it was observed that the SF added to the UHPC mixtures as a substitute for cement, resulted in a compressive strength value of 130 MPa or greater and flexural strength values (Fig. 6) of 19–24 MPa, highlighting the positive contribution of this additive to the properties of the concrete.

4.2. Results of Fire Resistance

Fire resistance tests were used to analyze the mechanical properties of the concrete and the results are shown in Table 5 for each compressive strength and flexural strength.

Used to determine the high-temperature effect , the compressive strength and flexural strength are important parameters of measured after it heated up to a certain temperature and the internal temperature of the material is brought to the ambient air temperature.. The results obtained during this phase of testing (Table 5) revealed little change in the strength of the samples up to a temperature of 300ºC. For certain groups, this temperature was even greater due to the additives used. However, depending on the materials used, at temperatures of 450ºC and greater, explosions that occurred in the samples caused structural damage (Fig. 7).

It was observed that temperature increases up to 300°C in the UHPCs caused the strength (compressive and flexural) to increase slightly (Fig. 8), however, the temperature was increased further, the samples experienced a significant loss of strength. The UHPC exhibited decomposition (Fig. 7) due to explosions in the samples caused by the intrinsic temperature increase in the furnace (temperatures of between 400°C and 600°C). Three stages were distinguished, with significant variations in the angle of the flexural strength. In the first stage, it was determined that the average compressive strength values did not decrease between 25°C and 300°C, and there was an increase of approximately 32.19% in the F20G20 mixture group and an average increase of 8–9% in all the mixture groups. These increases in the UHPC may have been due to the low water permeability that triggering the delayed strength increase.

Table 5

Compressive strength and flexural strength test results for mixtures

Mix code	25 °C		300 °C		450 °C		600 °C	
	CS (MPa)	FS (MPa)	CS (MPa)	FS (MPa)	CS (MPa)	FS (MPa)	CS (MPa)	FS (MPa)
Control	118.35	22.66	125.05	25.10	154.57	21.80	107.38	15.83
S0F10G10	94.28	22.03	103.66	22.76	122.29	23.27	113.94	15.42
S0F15G15	106.84	22.08	111.89	24.30	132.24	24.37	120.64	17.11
S0F20G20	106.21	21.94	140.40	24.14	148.30	21.94	132.54	14.25
S10F0G10	147.07	26.88	148.34	24.77	191.46	25.15	*	*
S10F10G0	139.32	26.27	146.89	17.55	*	*	*	*
S10F15G20	127.43	18.28	136.76	16.99	*	*	*	*
S10F20G15	121.83	18.31	118.52	11.84	*	*	*	*
S15F0G15	139.35	23.25	148.19	16.80	*	*	*	*
S15F10G20	115.05	19.48	152.06	18.56	*	*	*	*
S15F15G0	131.46	22.76	142.85	13.31	*	*	*	*
S15F20G10	123.17	15.89	148.70	17.70	*	*	*	*
S20F0G20	139.48	22.64	134.23	15.87	191.94	24.30	*	*
S20F10G15	130.91	21.75	138.23	23.84	144.78	21.70	*	*
S20F15G10	138.34	21.12	131.63	26.74	151.56	23.72	*	*
S20F20G0	133.50	22.52	152.33	25.34	183.33	20.98	*	*

*(CS) Compressive strength, (FS) Flexural strength, * Not measured*

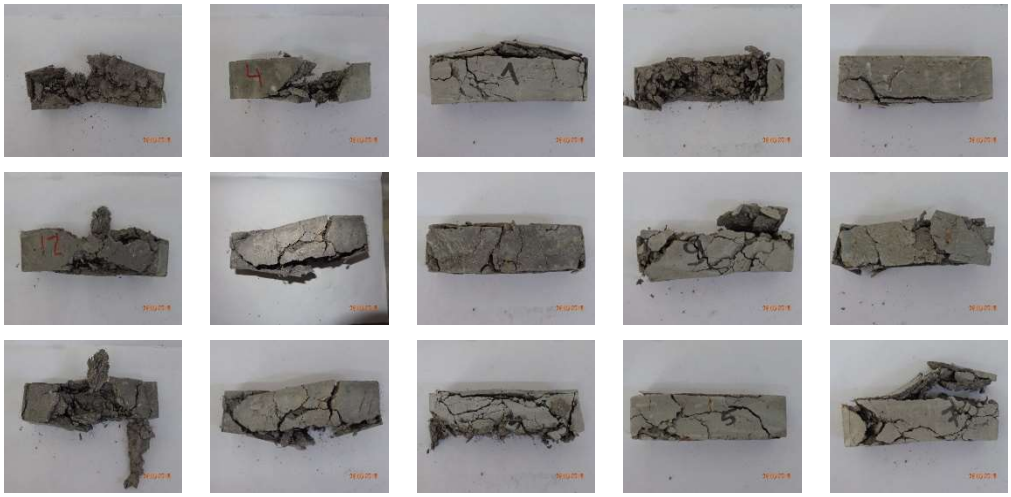

Fig. 7 - Sample damage at temperatures of 450 ° C and above

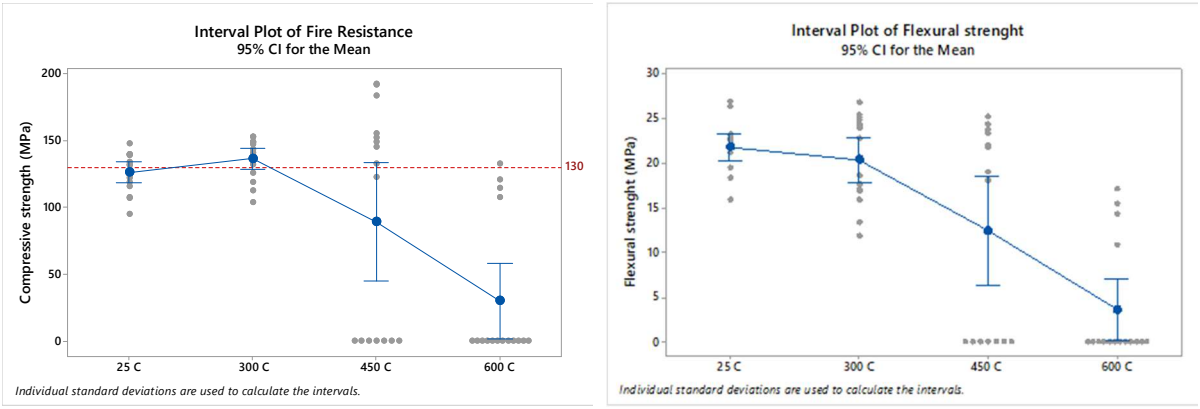

(a) (b)

Fig. 8 - Change of compressive strength loss (a) and flexural strength loss (b) at high temperature in UHPCs

Alternatively, the increases may have been associated with the water discharge that caused the concrete to shrink and created a more porous microstructure in the concrete. The increase in strength also coincides with the fact that high temperature accelerates the pozzolanic reaction, increases the hydration products and reduces the pore size [89]. During the second phase, under the effect of high temperature, although the compressive strength values between 300°C and 450°C increased in parallel with an increase in the temperature of several of the mixture groups, strength was not obtained in certain groups due to damage. In the third stage, at 600°C, the compressive strength did not increase in twelve of the mixtures, and the strength decreased compared to its value at 450°C for all groups. This can mostly be explained by thermal mismatches between the cement paste, or aggregates and cracks that occurred due to decomposition of the hydration products such as calcium-silica-hydrate (C-S-H) and calcium-hydroxide (C-H). Additionally, the steel fibers prevent cracking due to heat exposure and mechanical loading. No significant effect of the steel fibers on the flexural strength of the UHPC was observed.

The gradual heating of the UHPC up to 600°C resulted in a decrease in the flexural strength values (Fig. 8b and Table 5). However, although this decrease varied in the groups subjected to 300°C, a slight increase in the strength was observed in several groups. In contrast to this increase in the strength in several groups, the temperature increase caused a depreciation of up to 28% in the other groups and in all the groups in which the values could be measured at temperatures of 450°C or greater. However, the fact that this rate of decrease was less than the rate of compressive strength is considered positive. The loss of flexural strength occurred due to many micro and macro cracks that were produced in the specimens due to thermal incompatibility between the sand and cement paste [88].

The extremely high compressive strength and toughness properties of UHPC are mainly due to the increased mold settling density. However, an additional value that can be examined at high temperatures is whether there are mass losses. Table 6 and Figure 9 show the mass losses at 300°C, 450°C and 600°C for all the mixtures. The increasing density caused an increase in the sensitivity and an explosive effect due to a decrease in the porosity and dry-bulk density (Fig. 10). The

control mixture of the UHPC exhibited non-explosive decomposition up to 600°C at test temperatures. This was due to the addition of steel fibers to the concrete, which increased its thermal diffusivity by 50% to 100% [90], and the use of the fibers prevented the UHPC from flaking away.

Table 6

Mass loss results after exposure to high temperatures

Mix Code	Mass Loss (%) 300 °C	Mass Loss (%) 450 °C	Mass Loss (%) 600 °C
Control	0.15	0.60	5.80
S0F10G10	0.10	1.30	6.10
S0F15G15	0.15	1.80	5.80
S0F20G20	0.10	2.40	6.40
S10F0G10	0.15	4.40	3.40
S10F10G0	0.20	24.25	23.10
S10F15G20	0.25	5.30	6.00
S10F20G15	0.20	4.50	14.60
S15F0G15	0.40	11.40	13.90
S15F10G20	1.30	7.60	6.50
S15F15G0	0.65	10.80	35.80
S15F20G10	0.90	5.80	10.60
S20F0G20	1.40	3.80	6.30
S20F10G15	1.00	4.30	7.20
S20F15G10	0.50	3.10	15.30
S20F20G0	0.70	2.80	8.40

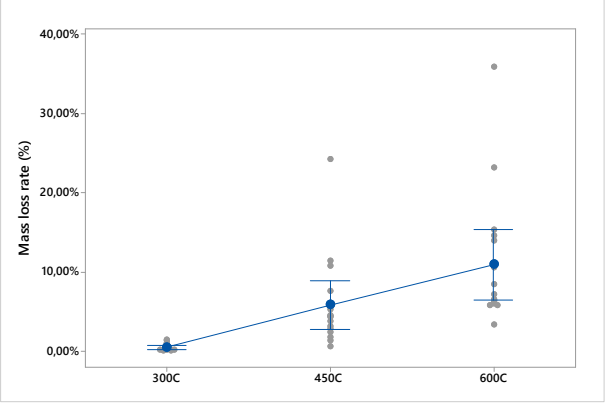

Fig. 9 - Change in mass losses after high temperature

An analysis of the effect of increasing temperatures on the loss of strength and mass in the samples demonstrated either a high density-low porosity relationship or a low density-high porosity relationship. An increased vacancy rate in the UHPCs helped to decrease the vapor pressure caused by the water at high temperatures. This also decreased the tendency of dense concretes to splinter or explode when heated rapidly [89,90]. In low-density concrete, the pressure generated is generally not severe due to the high pore volume, and the results of the present study corroborated this.

The effects of varying temperature levels on UHPCs were investigated, and the effects of the mineral additives (FA, GBFS and SF) on the mass-loss rate are shown in Figure 11. The mass-loss rate increased due to increasing temperatures if GBFS was not used. When GBFS was used at 300°C, it did not contribute to the mass loss rate, however, when it was used at temperatures of 450°C and 600°C, it caused a significant decrease in the mass-loss rate. The use of up to 10% of SF in the group that was exposed to 300°C did not affect the mass-loss rate, and it has caused a mass loss rate of approximately 1% for the other temperatures used. However, when 15% or greater of SF was used at 450°C and 20% of SF was used at 600°C, the rate of mass loss decreased. A similar situation was observed with the addition of FA. However, at 300°C the FA additive had almost no effect on reducing the mass-loss rate. Considering that the ideal temperature in terms of compressive strength was 450°C, it was observed that the most effective material for mass loss was GBFS, followed by SF and FA.

Statistical analyzes were also performed on the relationships between strength (CS), porosity (PO) and bulk density (BD) at elevated temperatures. The regression equation and significance levels showing the effect of increasing temperatures on UHPCs are given in Table 7. At a significance level of $P<0.05$, PO caused a statistical difference at 300 °C, whereas BD did not cause a difference at temperatures up to 600 °C. According to the increasing temperature values, the PO effect at 600 °C at a significance level of $P<0.05$ was less than the BD effect. This showed that the varying sample densities at high temperature were a statistically difference.

Table 7

Regression equation results at UHPCs

Temperature	Equation	P
300 °C	PO = 4,095 - 0,01825 . CS	0,00*
	BD = 2320,6 + 0,2670 . CS	0,483
450 °C	PO = 1,449 + 0,00181 . CS	0,095
	BD = 2369,47 - 0,1406 .CS	0,024*
600 °C	PO = 1,4776 + 0,00445 . CS	0,13
	BD = 2361,52 - 0,1528 . CS	0,04*

* P<0.05

4.3. Taguchi Optimization

The most ideal mixture was developed based on the results obtained using the Taguchi L16 test matrix. Firstly, the optimum results concerning the compressive and flexural strengths after exposure of the concrete to high temperatures are provided in Figures 12 and 13, and the optimum levels of these results are provided in Table 8.

The results revealed a total of four different mixture groups, one of which was the same as the L16 group and three were different to the L16 group. According to the Taguchi approach, the ideal optimum result of compressive strength for 300°C in the UHPCs was the S15F20G0 mixture group, in which 15% SF, 20% FA and 0% GBFS was used. It was observed that the ideal optimum result of the compressive strength for 450°C was the S20F0G10 mixture group, in which 20% SF, 0% FA and 10% GBFS was used. However, the optimum flexural strength was demonstrated by a mixture in the L16 group and included 0% SF, 10% FA and 10% GBFS

at 300°C. The optimum flexural strength at 450°C was the S0F0G10 mixture group which included 0% SF, 0% FA and 10% GBFS. The results obtained from validation experiments to control the values of the Taguchi optimization reflect the success of the optimization. Accordingly, the results demonstrated that the optimum conditions were estimated and the values obtained as a result of the calculations and verification experiments were reached (Table 9).

Table 8
Optimum Taguchi level and values for strength depending on curing conditions

Test	Control factors	Unit	Optimum level	Optimum value
Compressive strength for 300 °C	SF	%	3	15
	FA	%	4	20
	GBFS	%	1	0
Compressive strength for 450 °C	SF	%	4	20
	FA	%	1	0
	GBFS	%	2	10
Flexural strength for 300 °C	SF	%	1	0
	FA	%	2	10
	GBFS	%	2	10
Flexural strength for 450 °C	SF	%	1	0
	FA	%	1	0
	GBFS	%	2	10

Table 9
Optimal results and validation experiments for control factors

Test	Taguchi optimization	Predicted value			Real value		
		SF	FA	GBFS	SF	FA	GBFS
Compressive strength for 300 C	Level	3	4	1	3	4	1
	Value	15	20	0	15	20	0
	Result	157,25 MPa			148,37 MPa		
Compressive strength for 450 C	Level	4	1	2	4	1	2
	Value	20	0	10	20	0	10
	Result	169,19 MPa			154,17 MPa		
Flexural strength for 300 C	Level	1	2	2	1	2	2
	Value	0	10	10	0	10	10
	Result	27,04 MPa			27,04 MPa		
Flexural strength for 450 C	Level	1	1	2	1	1	2
	Value	0	0	10	0	0	10
	Result	28,50 MPa			26,18 MPa		

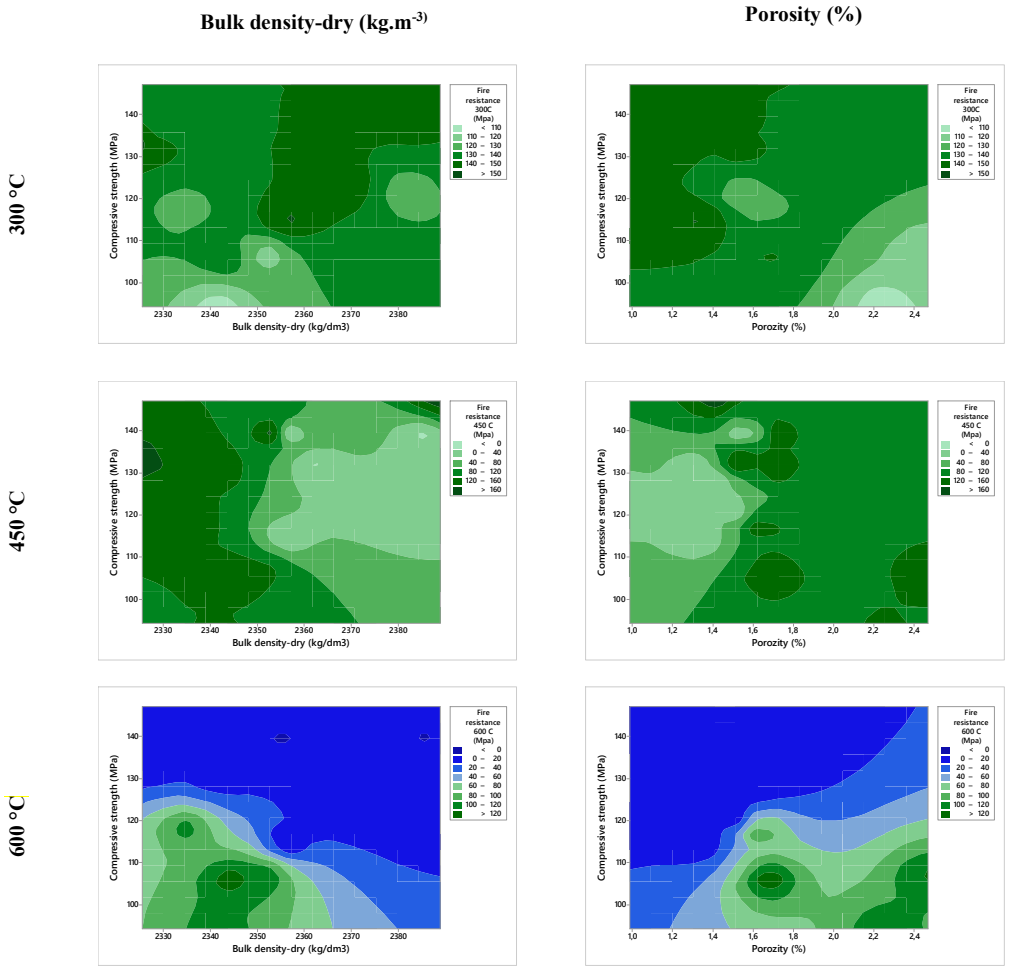

Fig. 10 - Contour plot of porosity and dry density results after high temperature

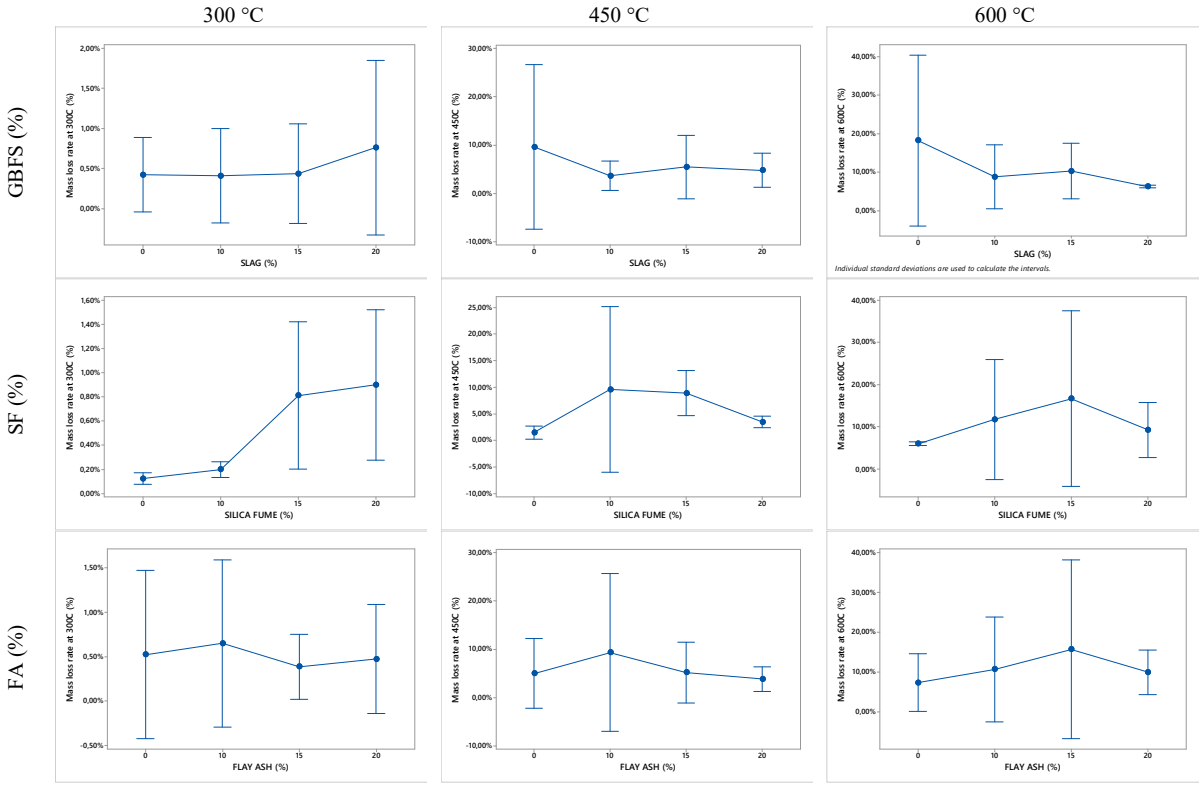

Fig. 11 - Effect of FA, GBFS and SF additive on change at high temperature

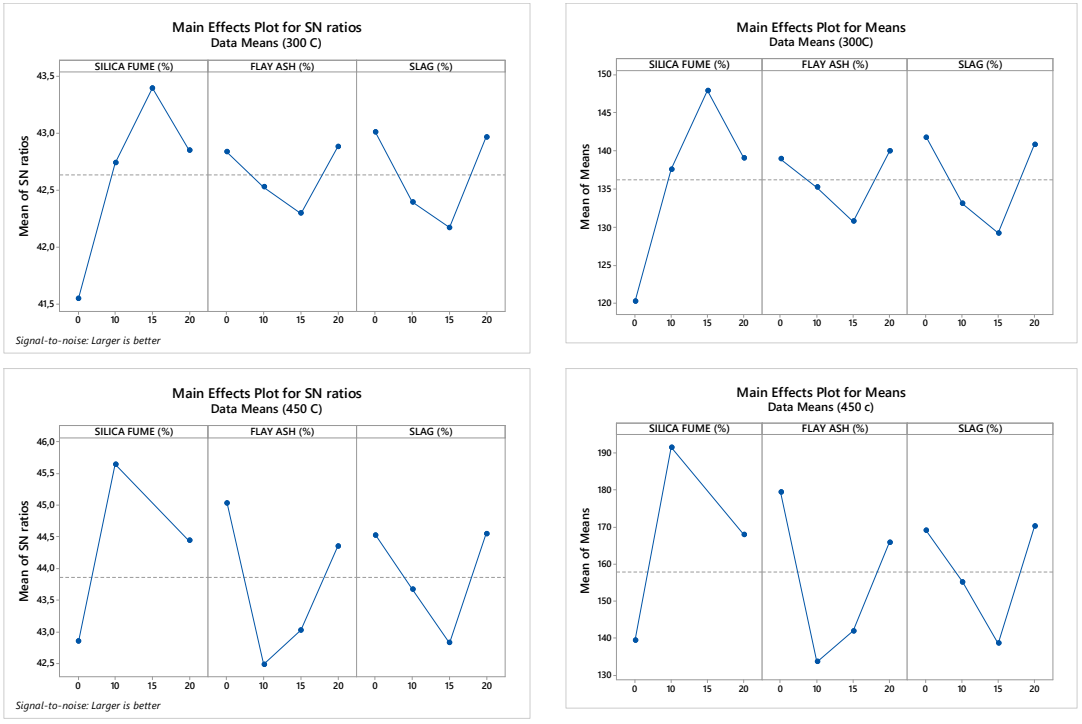

Fig. 12 - Taguchi optimization SN ratios and control factor graphs for compressive strength after high fire

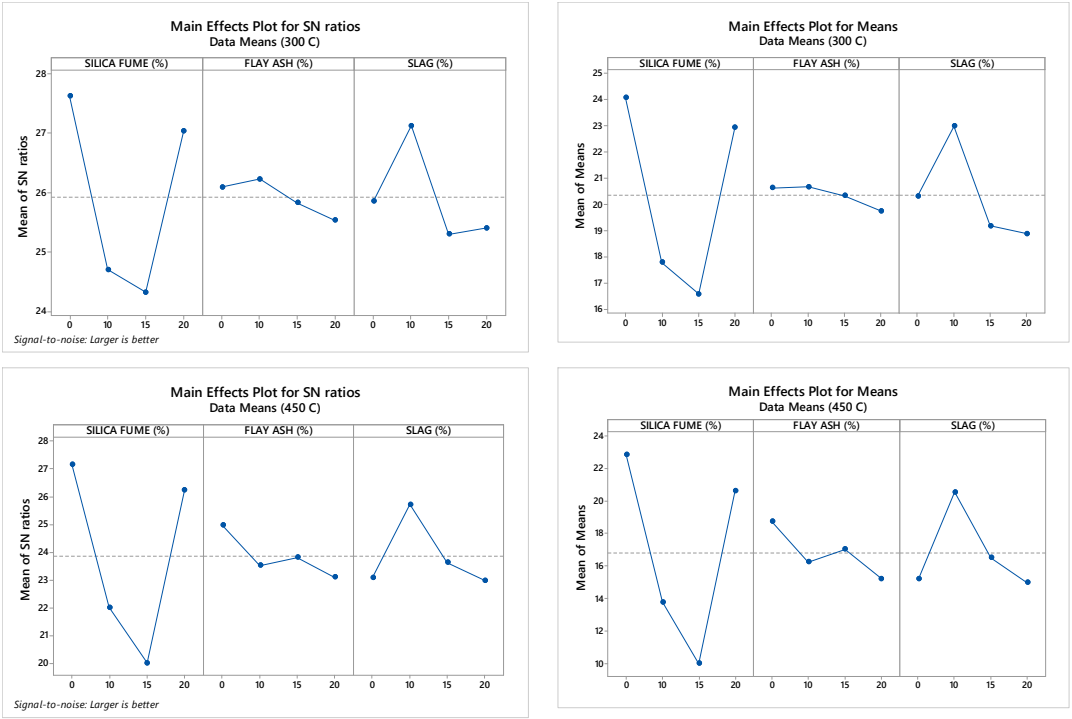

Fig. 13 - Taguchi optimization SN ratios and control factor graphs for flexural strength after high fire

5. Conclusions

The results obtained in this study by adding steel fibers, GBFS, FA and SF to the UHPCs are listed below:

- When Taguchi analysis was examined for compressive strength, the effect of the S/N ratios on the compressive strength was obtained at a mixture of 20% SF, 0% FA and 10% GBFS and a maximum compressive strength was obtained at 450°C.
- Taguchi analysis for flexural strength was obtained in a mixture of 0% SF, 0% FA and 10% GBFS at had an optimum level at 450°C.
- The results of an examination of the effect of high temperatures on UHPCs showed that the compressive strength did not decrease between 25°C and 300°C, and there was an increase of approximately 32.19% in the F20G20 mixture. Furthermore, an average increase in the compressive strength of 8–9% was observed for all mixtures. It was observed that between approximately 300°C and 450°C, several mixtures began to degrade, and the increase in the compressive strength continued in other groups with an increase in the temperature. It was determined that the high-temperature effect in the UHPCs was more effective at temperatures of 600°C and greater, and twelve of the mixtures were damaged due to degradation.
- An examination of the values obtained in the verification test demonstrated that the results were sufficient concerning the compressive and flexural strength and physical properties under various heating conditions and that the Taguchi optimization can be successfully applied

Acknowledgements

This study was presented by Ali Alshaab Ramroom as a master thesis at Kastamonu University, Institute of Science.

There is no conflict of interest between the authors on any issue.

REFERENCES

[1] A. Alsalman, C.N. Dang, J.R. Martí-Vargas, W. Micah Hale, Mixture-proportioning of economical UHPC mixtures, J. Build. Eng. 27, 2020. https://doi.org/10.1016/j.jobe.2019.100970.

[2] M. Najimi, J. Sobhani, B. Ahmadi, M. Shekarchi, An experimental study on durability properties of concrete containing zeolite as a highly reactive natural pozzolan, Constr. Build. Mater. 35, 2012. 1023–1033. https://doi.org/10.1016/j.conbuildmat.2012.04.038.

[3] H. Eskandari, M. Vaghefi, K. Kowsari, Investigation of Mechanical and Durability Properties of Concrete Influenced by Hybrid Nano Silica and Micro Zeolite, Procedia Mater. Sci. 11, 2015. 594–599. https://doi.org/10.1016/j.mspro.2015.11.084.

[4] W. Wang, J. Liu, F. Agostini, C.A. Davy, F. Skoczylas, D. Corvez, Durability of an Ultra High Performance Fiber Reinforced Concrete (UHPFRC) under progressive aging, Cem. Concr. Res. 55, 2014. 1–13. https://doi.org/10.1016/j.cemconres.2013.09.008.

[5] D.Y. Yoo, N. Banthia, Mechanical properties of ultra-high-performance fiber-reinforced concrete: A review, Cem. Concr. Compos. 73, 2016. 267–280. https://doi.org/10.1016/j.cemconcomp.2016.08.001.

[6] R. Yu, L. Van Beers, P. Spiesz, H.J.H. Brouwers, Impact resistance of a sustainable Ultra-High Performance Fibre Reinforced Concrete (UHPFRC) under pendulum impact loadings, Constr. Build. Mater. 107, 2016. 203–215. https://doi.org/10.1016/j.conbuildmat.2015.12.157.

[7] S. Memiş, S. Şahin, Ü. Şirin, Some properties of prefabricated building materials produced from ground diatomite and hydrophone clay, Pamukkale Univ Muh Bilim Derg. 23, 2017. 245–249. https://doi.org/10.5505/pajes.2016.34467.

[8] G. Kaplan, S.A. Yildizel, S. Memiş, A.U. Öztürk, The Optimization of Calcareous Fly Ash-Added Cement Containing Grinding Aids and Strength-Improving Additives, Adv. Civ. Eng., 2018. https://doi.org/10.1155/2018/8917059.

[9] S. Memis, S. Sahin, Investigation of the effect of press compaction and the use of zeolite on mechanical properties in the production of low strength Reactive Powder Concrete (RPC), Fresenius Environ. Bull. 28, 2019.

[10] G. Kaplan, H. Yaprak, S. Memiş, A. Alnkaa, Artificial neural network estimation of the effect of varying curing conditions and cement type on hardened concrete properties, Buildings. 9, 2019. https://doi.org/10.3390/buildings9010010.
[11] X. Liang, C. Wu, Y. Yang, Z. Li, Experimental study on ultra-high performance concrete with high fire resistance under simultaneous effect of elevated temperature and impact loading, Cem. Concr. Compos. 98, 2019. 29–38. https://doi.org/10.1016/j.cemconcomp.2019.01.017.
[12] J. Li, Z. Wu, C. Shi, Q. Yuan, Z. Zhang, Durability of ultra-high performance concrete – A review, Constr. Build. Mater. 255, 2020. 119296. https://doi.org/10.1016/j.conbuildmat.2020.119296.
[13] L.A. Sbia, A. Peyvandi, J. Lu, S. Abideen, R.R. Weerasiri, A.M. Balachandra, P. Soroushian, Production methods for reliable construction of ultra-high-performance concrete (UHPC) structures, Mater. Struct. Constr. 50, 2017. 1–19. https://doi.org/10.1617/s11527-016-0887-4.
[14] V. Kodur, S. Banerji, R. Solhmirzaei, Effect of Temperature on Thermal Properties of Ultrahigh-Performance Concrete, J. Mater. Civ. Eng. 32, 2020. 04020210. https://doi.org/10.1061/(asce)mt.1943-5533.0003286.
[15] O.M. Abdulkareem, A. Ben Fraj, M. Bouasker, A. Khelidj, Mixture design and early age investigations of more sustainable UHPC, Constr. Build. Mater. 163, 2018. 235–246. https://doi.org/10.1016/j.conbuildmat.2017.12.107.
[16] R. Yu, P. Spiesz, H.J.H. Brouwers, Development of an eco-friendly Ultra-High Performance Concrete (UHPC) with efficient cement and mineral admixtures uses, Cem. Concr. Compos. 55, 2015. 383–394. https://doi.org/10.1016/j.cemconcomp.2014.09.024.
[17] N. Behzad, S.M.R. Raizal, J.M. Saleh, Y.L. Voo, A review on ultra high performance'ductile'concrete (UHPdC) technology, Int. J. Civ. \& Struct. Eng. 2, 2012. 1003.
[18] W. Meng, M. Valipour, K.H. Khayat, Optimization and performance of cost-effective ultra-high performance concrete, Mater. Struct. Constr. 50, 2017. 1–16. https://doi.org/10.1617/s11527-016-0896-3.
[19] Z. Wu, K.H. Khayat, C. Shi, Changes in rheology and mechanical properties of ultra-high performance concrete with silica fume content, Cem. Concr. Res. 123, 2019. 105786. https://doi.org/10.1016/j.cemconres.2019.105786.
[20] ACI 239R-18, Ultra-High-Performance Concrete: An Emerging Technology Report. Front Cover. ACI Committee 239., 2018.
[21] ASTM C1856 / C1856M - 17, Standard Practice for Fabricating and Testing Specimens of Ultra-High Performance Concrete aggregate size, 2017.
[22] D. Hou, D. Wu, X. Wang, S. Gao, R. Yu, M. Li, P. Wang, Y. Wang, Sustainable use of red mud in ultra-high performance concrete (UHPC): Design and performance evaluation, Cem. Concr. Compos. 115, 2021. https://doi.org/10.1016/j.cemconcomp.2020.103862.
[23] B.A. Graybeal, H.G. Russel, Ultra-High Performance Concrete: A State-of-the-Art Report for the Bridge Community. Publication N.º FHWA-HRT-13-060, 2013. 176.
[24] N.K. Lee, K.T. Koh, S.H. Park, G.S. Ryu, Microstructural investigation of calcium aluminate cement-based ultra-high performance concrete (UHPC) exposed to high temperatures, Cem. Concr. Res. 102, 2017. 109–118. https://doi.org/10.1016/j.cemconres.2017.09.004.
[25] M.R. Moallem, Flexural Redistribution in Ultra-High Performance Concrete Lab Specimens, Ohio University, 2010.
[26] R. Yu, Development of sustainable protective ultra-high performance fibre reinforced concrete (UHPFRC) : design, assessment and modeling, Technische Universiteit Eindhoven, 2015.
[27] R.N. Maten, Ultra High Performance Concrete in Large Span Shell Structures, 2011. 266.
[28] X. Liang, C. Wu, Y. Su, Z. Chen, Z. Li, Development of ultra-high performance concrete with high fire resistance, Constr. Build. Mater. 2018. 400–412.
[29] F. Toutlemonde, J. Resplendino, Designing and Building with UHPFRC, Wiley, 2013. https://doi.org/10.1002/9781118557839.
[30] H. Russel, G, B. a. Graybeal, Ultra-High Performance Concrete : A State-of-the-Art Report for the Bridge Community, Federal Highway Administration, United States, 2013.
[31] M.B. Eide, J.-M. Hisdal, Ultra High Performance Fibre Reinforced Concrete (UHPFRC) – State of the art, Cooperation partners, 2012.
[32] B. Li, H. Li, M. Siahkouhi, G. Jing, Study on Coupling of Glass Powder and Steel Fiber as Silica Fume Replacement in Ultra-High Performance Concrete: Concrete Sleeper Admixture Case Study, KSCE J. Civ. Eng. 24, 2020. 1545–1556. https://doi.org/10.1007/s12205-020-0832-5.
[33] A. Wetzel, B. Middendorf, Influence of silica fume on properties of fresh and hardened ultra-high performance concrete based on alkali-activated slag, Cem. Concr. Compos. 100, 2019. 53–59. https://doi.org/10.1016/j.cemconcomp.2019.03.023.
[34] M. Schleiting, A. Wetzel, P. Krooß, J. Thiemicke, T. Niendorf, B. Middendorf, E. Fehling, Functional microfibre reinforced ultra-high performance concrete (FMF-UHPC), Cem. Concr. Res. 130, 2020. 105993. https://doi.org/10.1016/j.cemconres.2020.105993.
[35] A. Arora, A. Almujaddidi, F. Kianmofrad, B. Mobasher, N. Neithalath, Material design of economical ultra-high performance concrete (UHPC) and evaluation of their properties, Cem. Concr. Compos. 104, 2019. 103346. https://doi.org/10.1016/j.cemconcomp.2019.103346.
[36] L. Teng, J. Zhu, K.H. Khayat, J. Liu, Effect of welan gum and nanoclay on thixotropy of UHPC, Cem. Concr. Res. 138. 2020, 106238. https://doi.org/10.1016/j.cemconres.2020.106238.
[37] M. Alkaysi, S. El-Tawil, Effects of variations in the mix constituents of ultra high performance concrete (UHPC) on cost and performance, Mater. Struct. Constr. 49, 2016. 4185–4200. https://doi.org/10.1617/s11527-015-0780-6.
[38] R. Yu, P. Spiesz, H.J.H. Brouwers, Mix design and properties assessment of Ultra-High Performance Fibre Reinforced Concrete (UHPFRC), Cem. Concr. Res. 56, 2014. 29–39. https://doi.org/10.1016/j.cemconres.2013.11.002.
[39] C. Wang, C. Yang, F. Liu, C. Wan, X. Pu, Preparation of Ultra-High Performance Concrete with common technology and materials, Cem. Concr. Compos. 34, 2012. 538–544. https://doi.org/10.1016/j.cemconcomp.2011.11.005.
[40] Z. Wu, C. Shi, K.H. Khayat, Influence of silica fume content on microstructure development and bond to steel fiber in ultra-high strength cement-based materials, Cem. Concr. Compos. 71, 2016, 97–109. https://doi.org/10.1016/j.cemconcomp.2016.05.005.
[41] Z. Wu, K.H. Khayat, C. Shi, Effect of nano-SiO2 particles and curing time on development of fiber-matrix bond properties and microstructure of ultra-high strength concrete, Cem. Concr. Res. 95, 2017. 247–256. https://doi.org/10.1016/j.cemconres.2017.02.031.
[42] M. Ipek, K. Yilmaz, M. Uysal, The effect of pre-setting pressure applied flexural strength and fracture toughness of reactive powder concrete during the setting phase, Constr. Build. Mater. 26, 2012. 459–465. https://doi.org/10.1016/j.conbuildmat.2011.06.045.
[43] M. Ipek, K. Yilmaz, M. Sümer, M. Saribiyik, Effect of pre-setting pressure applied to mechanical behaviours of reactive powder concrete during setting phase, Constr. Build. Mater. 25, 2011. 61–68. https://doi.org/10.1016/j.conbuildmat.2010.06.056.
[44] B. Tutkun, H. Yazıcı, Evaluation of enhanced autogenous self-healing ability of UHPC mixtures, 280, 2021. https://doi.org/10.1016/j.conbuildmat.2021.122524.
[45] S. Memiş, A.A. Ramroom, Investigation of the ideal mixing ratio and steel fiber additive in ultra high performance concrete (Uhpc), Rev. Rom. Mater. Rom. J. Mater. 50, 2020. 403–410.
[46] T. Xie, C. Fang, M.S. Mohamad Ali, P. Visintin, Characterizations of autogenous and drying shrinkage of ultra-high performance concrete (UHPC): An experimental study, Cem. Concr. Compos. 91, 2018. 156–173. https://doi.org/10.1016/j.cemconcomp.2018.05.009.
[47] Z. Wu, C. Shi, K.H. Khayat, Investigation of mechanical properties and shrinkage of ultra-high performance concrete: Influence of steel fiber content and shape, Compos. Part B Eng. 174, 2019. 107021. https://doi.org/10.1016/j.compositesb.2019.107021.
[48] J. Justs, M. Wyrzykowski, D. Bajare, P. Lura, Internal curing by superabsorbent polymers in ultra-high performance concrete, Cem. Concr. Res. 76, 2015. 82–90. https://doi.org/10.1016/j.cemconres.2015.05.005.
[49] L. Yu, L. Huang, H. Ding, Rheological and mechanical properties of ultra-high-performance concrete containing fine recycled concrete aggregates, Materials (Basel). 12, 2019. https://doi.org/10.3390/ma12223717.
[50] L. Teng, M. Valipour, K.H. Khayat, Design and performance of low shrinkage UHPC for thin bonded bridge deck overlay, Cem. Concr. Compos., 2021. 103953. https://doi.org/10.1016/j.cemconcomp.2021.103953.
[51] X. Zhang, Z. Liu, F. Wang, Autogenous shrinkage behavior of ultra-high performance concrete, Constr. Build. Mater. 226, 2019. 459–468. https://doi.org/10.1016/j.conbuildmat.2019.07.177.
[52] A.A. Semendary, W.K. Hamid, E.P. Steinberg, I. Khoury, Shear friction performance between high strength concrete (HSC) and ultra high performance concrete (UHPC) for bridge connection applications, Eng. Struct. 205, 2020. 110122. https://doi.org/10.1016/j.engstruct.2019.110122.
[53] X. Wang, R. Yu, Z. Shui, Q. Song, Z. Liu, M. bao, Z. Liu, S. Wu, Optimized treatment of recycled construction and demolition waste in developing sustainable ultra-high performance concrete, J. Clean. Prod. 221, 2019. 805–816.

[54] M.G. Sohail, R. Kahraman, N. Al Nuaimi, B. Gencturk, W. Alnahhal, Durability characteristics of high and ultra-high performance concretes, J. Build. Eng. 33, 2021. 101669. https://doi.org/10.1016/j.jobe.2020.101669

[55] S.H. Kang, S.G. Hong, J. Moon, The use of rice husk ash as reactive filler in ultra-high performance concrete, Cem. Concr. Res. 115, 2019. 389–400. https://doi.org/10.1016/j.cemconres.2018.09.004.

[56] Ç. Yalçınkaya, O. Çopuroğlu, Hydration heat, strength and microstructure characteristics of UHPC containing blast furnace slag, J. Build. Eng. 34, 2021. https://doi.org/10.1016/j.jobe.2020.101915.

[57] R. Yu, P. Spiesz, H.J.H. Brouwers, Effect of nano-silica on the hydration and microstructure development of Ultra-High Performance Concrete (UHPC) with a low binder amount, Constr. Build. Mater. 65, 2014. 140–150. https://doi.org/10.1016/j.conbuildmat.2014.04.063.

[58] Y. Bae, S. Pyo, Ultra high performance concrete (UHPC) sleeper: Structural design and performance, Eng. Struct. 210, 2020. 110374. https://doi.org/10.1016/j.engstruct.2020.110374.

[59] N. Naeimi, M.A. Moustafa, Compressive behavior and stress–strain relationships of confined and unconfined UHPC, Constr. Build. Mater. 272, 2021. 121844. https://doi.org/10.1016/j.conbuildmat.2020.121844.

[60] L. Tong, L. Chen, M. Wen, C. Xu, Static behavior of stud shear connectors in high-strength-steel–UHPC composite beams, Eng. Struct. 218, 2020. 110827. https://doi.org/10.1016/j.engstruct.2020.110827.

[61] F. Dingqiang, R. Yu, L. Kangning, T. Junhui, S. Zhonghe, W. Chunfeng, W. Shuo, G. Zhenfeng, H. Zhengdong, S. Qiqi, Optimized design of steel fibres reinforced ultra-high performance concrete (UHPC) composites: Towards to dense structure and efficient fibre application, Constr. Build. Mater. 273, 2020. 121698. https://doi.org/10.1016/j.conbuildmat.2020.121698.

[62] M.M. Reda, N.G. Shrive, J.E. Gillott, Microstructural investigation of innovative UHPC, Cem. Concr. Res. 29, 1999. 323–329. https://doi.org/10.1016/S0008-8846(98)00225-7.

[63] O.M. Abdulkareem, A. Ben Fraj, M. Bouasker, A. Khelidj, Effect of chemical and thermal activation on the microstructural and mechanical properties of more sustainable UHPC, Constr. Build. Mater. 169, 2018. 567–577. https://doi.org/10.1016/j.conbuildmat.2018.02.214.

[64] Y. Zhang, S. Cai, Y. Zhu, L. Fan, X. Shao, Flexural responses of steel-UHPC composite beams under hogging moment, Eng. Struct. 206, 2020. 110134. https://doi.org/10.1016/j.engstruct.2019.110134.

[65] J.L. Provis, A. Palomo, Advances in understanding alkali-activated materials, Cem. Concr. Res. 78, 2015. 110–125. https://doi.org/10.1016/J.CEMCONRES.2015.04.013.

[66] H. Hardjasaputra, V. Indrawati, I. Djohari, STUDY TO IMPROVE FIRE RESISTANCE OF ULTRA HIGH PERFORMANCE CONCRETE BY CONDUCTING FIRE TESTS OF UHPC CYLINDER SPECIMENS IN, (n.d.) 13–18.

[67] R.K. Roy, A Primer on the Taguchi Method, Society of Manufacturing Engineers, 1990.

[68] M. Nuruddin, R. Bayuaji, Application of Taguchi's approach in the optimization of mix proportion for Microwave Incinerated Rice Husk Ash foamed concrete, Ijcee. 9, 2009. 121–129.

[69] M.F.B. Nuruddin, R. Bayuji, Optimum Mix Proportioning of Mirha Foamed Concrete Using Taguchi ' S Approach, Apsec-Eacef. 2009, 694–700.

[70] I. Türkmen, R. Gül, C. Çelik, A Taguchi approach for investigation of some physical properties of concrete produced from mineral admixtures, Build. Environ. 43, 2008. 1127–1137. https://doi.org/10.1016/j.buildenv.2007.02.005.

[71] ASTM C 136 / C136M-19, Standard Test Method for Sieve Analysis of Fine and Coarse Aggregates, ASTM Int. 2014.

[72] TS EN 197-1, Cement--Part 1: compositions and conformity criteria for common cements, Turkish Stand. Inst. 2002.

[73] M. AASHTO, 307 ASTM C 1240."Standard Specification for Silica Fume Used in Cementitious Mixtures," Am. Soc. Test. Mater. Annu. B. ASTM Stand. Vol. 2 (n.d.).

[74] ASTM C618, Standard specification for coal fly ash and raw or calcined natural pozzolan for use in concrete. American society for testing and materials. West Conshohocken, PA, USA: ASTM International, ASTM Int. 2003.

[75] T. Hirata, J. Ye, P. Branicio, J. Zheng, A. Lange, J. Plank, M. Sullivan, Adsorbed Conformations of PCE Superplasticizers in Cement Pore Solution Unraveled by Molecular Dynamics Simulations, Sci. Rep. 7, 2017. 16599. https://doi.org/10.1038/s41598-017-16048-3.

[76] E. Fehling, M. Schmidt, S. Stürwald, Ultra High Performance Concrete (UHPC): Proceedings of the Second International Symposium on Ultra High Performance Concrete, Kassel, Germany, March 05-07, 2008, kassel university press GmbH, 2008.

[77] E.C. Torregrosa, Dosage optimization and bolted connections for UHPFRC ties - [Thesis], Riunet. 2013. 1–276.

[78] D. Wang, C. Shi, Z. Wu, J. Xiao, Z. Huang, Z. Fang, A review on ultra high performance concrete: Part II. Hydration, microstructure and properties, Constr. Build. Mater. 96, 2015. 368–377. https://doi.org/10.1016/j.conbuildmat.2015.08.095.

[79] R. Christ, F. Pacheco, H. Ehrenbring, U. Quinino, M. Mancio, Y. Muñoz, B. Tutikian, Study of mechanical behavior of ultra - High performance concrete (UHPC) reinforced with hybrid fibers and with reduced cement consumption, Rev. Ing. Constr. 34, 2019. 159–168. https://doi.org/10.4067/S0718-50732019000200159.

[80] B. Chun, D.Y. Yoo, Hybrid effect of macro and micro steel fibers on the pullout and tensile behaviors of ultra-high-performance concrete, Compos. Part B Eng. 162, 2019. 344–360. https://doi.org/10.1016/j.compositesb.2018.11.026.

[81] P.P. Li, Q.L. Yu, H.J.H. Brouwers, Effect of PCE-type superplasticizer on early-age behaviour of ultra-high performance concrete (UHPC), Constr. Build. Mater. 153, 2017. 740–750. https://doi.org/10.1016/j.conbuildmat.2017.07.145.

[82] S.H. Chu, A.K.H. Kwan, Mixture design of self-levelling ultra-high performance FRC, Constr. Build. Mater. 228, 2019. 116761. https://doi.org/10.1016/j.conbuildmat.2019.116761.

[83] C. Shi, Y.L. Mo, High-performance Construction Materials: Science and Applications, World Scientific, 2008.

[84] P.R. Prem, B.H. Bharatkumar, N.R. Iyer, Influence of curing regimes on compressive strength of ultra high performance concrete, Sadhana - Acad. Proc. Eng. Sci. 38, 2013. 1421–1431. https://doi.org/10.1007/s12046-013-0159-8.

[85] ASTM C192 / C192M-19, Standard Practice for Making and Curing Concrete Test Specimens in the Laboratory, ASTM International, West Conshohocken, PA, ASTM Int. 2019.

[86] BS EN 196-1, British Standard Methods of testing cement —, 3 2005.

[87] ASTM C642, Standard Test Method for Density , Absorption , and Voids in Hardened Concrete 1, 1997. 1–3.

[88] ASTM E831, Standard Test Method for Linear Thermal Expansion of Solid Materials by Thermomechanical Analysis, 2014.

[89] Tahwia, Performance of Ultra-High Performance Fiber Reinforced Concrete at High Temperatures, Int. J. Eng. Innov. Technol. 2017. 1–7.

[90] G.F. Peng, Q. Ma, H.M. Hu, R. Gao, Q.F. Yao, Y.F. Liu, The effects of air entrainment and pozzolans on frost resistance of 50-60 MPa grade concrete, Constr. Build. Mater. 21, 2007. 1034–1039. https://doi.org/10.1016/j.conbuildmat.2006.02.00

****